

This is a repository copy of *Recent Asian origin of chytrid fungi causing global amphibian declines*.

White Rose Research Online URL for this paper:
<https://eprints.whiterose.ac.uk/132755/>

Version: Accepted Version

Article:

O'Hanlon, Simon J., Rieux, Adrien, Farrer, Rhys A. et al. (55 more authors) (2018) Recent Asian origin of chytrid fungi causing global amphibian declines. *Science*. pp. 621-627.
ISSN 0036-8075

<https://doi.org/10.1126/science.aar1965>

Reuse

Items deposited in White Rose Research Online are protected by copyright, with all rights reserved unless indicated otherwise. They may be downloaded and/or printed for private study, or other acts as permitted by national copyright laws. The publisher or other rights holders may allow further reproduction and re-use of the full text version. This is indicated by the licence information on the White Rose Research Online record for the item.

Takedown

If you consider content in White Rose Research Online to be in breach of UK law, please notify us by emailing eprints@whiterose.ac.uk including the URL of the record and the reason for the withdrawal request.

1 **Title:** Recent Asian origin of chytrid fungi causing global amphibian declines *

2 **Authors:** Simon J. O'Hanlon^{1,2*}, Adrien Rieux³, Rhys A. Farrer¹, Gonçalo M. Rosa^{2,4,5},
 3 Bruce Waldman⁶, Arnaud Bataille^{6,7}, Tiffany A. Kosch^{8,6}, Kris A. Murray¹, Balázs
 4 Brankovics^{9,10}, Matteo Fumagalli^{11,31}, Michael D. Martin^{12,13}, Nathan Wales¹³, Mario
 5 Alvarado-Rybak¹⁴, Kieran A. Bates^{1,2}, Lee Berger⁸, Susanne Böll¹⁵, Lola Brookes², Frances
 6 Clare^{1,2}, Elodie A. Courtois¹⁶, Andrew A. Cunningham², Thomas M. Doherty-Bone¹⁷, Pria
 7 Ghosh^{1,18}, David J. Gower¹⁹, William E. Hintz²⁰, Jacob Höglund²¹, Thomas S. Jenkinson²²,
 8 Chun-Fu Lin²³, Anssi Laurila²¹, Adeline Loyau^{24,25}, An Martel²⁶, Sara Meurling²¹, Claude
 9 Miaud²⁷, Pete Minting²⁸, Frank Pasmans²⁶, Dirk Schmeller^{24,25}, Benedikt R. Schmidt²⁹,
 10 Jennifer M. G. Shelton¹, Lee F. Skerratt⁸, Freya Smith^{2,30}, Claudio Soto-Azat¹⁴, Matteo
 11 Spagnoletti³¹, Giulia Tessa³², Luís Felipe Toledo³³, Andrés Valenzuela-Sánchez^{34,14}, Ruhan
 12 Verster¹⁸, Judit Vörös³⁵, Rebecca J. Webb⁸, Claudia Wierzbicki¹, Emma Wombwell², Kelly
 13 R. Zamudio³⁶, David M. Aanensen^{37,1}, Timothy Y. James²², M. Thomas P. Gilbert^{13,12}, Ché
 14 Weldon¹⁸, Jaime Bosch³⁸, François Balloux³¹†, Trenton W. J. Garner^{2,18,32}†, Matthew C.
 15 Fisher^{1*}

16 **Affiliations:**

17 ¹ Department of Infectious Disease Epidemiology and MRC Centre for Global Infectious
 18 Disease Analysis, School of Public Health, Imperial College London, Norfolk Place, London
 19 W2 1PG, UK

20 ² Institute of Zoology, Regent's Park, London, NW1 4RY, UK

21 ³ CIRAD, UMR PVBMT, 97410 St Pierre, Reunion, France⁴ Department of Biology,
 22 University of Nevada, Reno, Reno NV 89557, USA

23 ⁵ Centre for Ecology, Evolution and Environmental Changes (CE3C), Faculdade de Ciências
 24 da Universidade de Lisboa, Lisboa, Portugal

25 ⁶ Laboratory of Behavioral and Population Ecology, School of Biological Sciences, Seoul
 26 National University, Seoul 08826, South Korea

27 ⁷ CIRAD, UMR ASTRE, F-34398 Montpellier, France

28 ⁸ One Health Research Group, College of Public Health, Medical and Veterinary Sciences,
 29 James Cook University, Townsville, Queensland, 4811, Australia

30 ⁹ Westerdijk Fungal Biodiversity Institute, Uppsalalaan 8, 3584CT Utrecht, The Netherlands

31 ¹⁰ Institute of Biodiversity and Ecosystem Dynamics, University of Amsterdam, Science Park
 32 904, 1098 XH Amsterdam, The Netherlands

33 ¹¹ Department of Life Sciences, Silwood Park Campus, Imperial College London, Ascot, UK

34 ¹² Department of Natural History, NTNU University Museum, Norwegian University of
 35 Science and Technology (NTNU), Erling Skakkes gate 49, NO-7012 Trondheim, Norway

36 ¹³ Centre for GeoGenetics, Natural History Museum of Denmark, University of Copenhagen,
 37 Øster Voldgade 5-7, 1350 Copenhagen, Denmark

38 ¹⁴ Centro de Investigación para la Sustentabilidad, Facultad de Ecología y Recursos
 39 Naturales, Universidad Andres Bello, Republica 440, Santiago, Chile

* This manuscript has been accepted for publication in Science. This version has not undergone final editing. Please refer to the complete version of record at <http://www.sciencemag.org/>. The manuscript may not be reproduced or used in any manner that does not fall within the fair use provisions of the Copyright Act without the prior, written permission of AAAS.

- 40 ¹⁵ Agency for Population Ecology and Nature Conservancy, Gerbrunn
 41 ¹⁶ Laboratoire Ecologie, évolution, interactions des systèmes amazoniens (LEEISA),
 42 Université de Guyane, CNRS, IFREMER, 97300 Cayenne, French Guiana.
 43 ¹⁷ Conservation Programmes, Royal Zoological Society of Scotland, Edinburgh, UK
 44 ¹⁸ Unit for Environmental Sciences and Management, Private Bag x6001, North-West
 45 University, Potchefstroom, 2520, South Africa
 46 ¹⁹ Life Sciences, The Natural History Museum, London SW7 5BD, UK
 47 ²⁰ Biology Department, University of Victoria, Victoria, BC, V8W 3N5, Canada
 48 ²¹ Department of Ecology and Genetics, EBC, Uppsala University. Norbyv. 18D, SE-75236,
 49 Uppsala, Sweden
 50 ²² Department of Ecology and Evolutionary Biology, University of Michigan, Ann Arbor,
 51 MI, 48109, USA
 52 ²³ Zoology Division, Endemic Species Research Institute, 1 Ming-shen East Road, Jiji,
 53 Nantou 552, Taiwan
 54 ²⁴ Helmholtz Centre for Environmental Research – UFZ, Department of Conservation
 55 Biology, Permoserstrasse 15, 04318 Leipzig, Germany
 56 ²⁵ EcoLab, Université de Toulouse, CNRS, INPT, UPS, Toulouse, France
 57 ²⁶ Department of Pathology, Bacteriology and Avian Diseases, Faculty of Veterinary
 58 Medicine, Ghent University, Salisburylaan 133, B-9820 Merelbeke, Belgium
 59 ²⁷ PSL Research University, CEFE UMR 5175, CNRS, Université de Montpellier, Université
 60 Paul-Valéry Montpellier, EPHE, Montpellier, France
 61 ²⁸ Amphibian and Reptile Conservation (ARC) Trust, 655A Christchurch Road, Boscombe,
 62 Bournemouth, Dorset, UK, BH1 4AP
 63 ²⁹ Department of Evolutionary Biology and Environmental Studies, University of Zurich,
 64 Winterthurerstrasse 190, 8057 Zurich, Switzerland and Info Fauna Karch, UniMail -
 65 Bâtiment G, Bellevaux 51, 2000 Neuchâtel, Switzerland
 66 ³⁰ National Wildlife Management Centre, APHA, Woodchester Park, Gloucestershire GL10
 67 3UJ, UK
 68 ³¹ UCL Genetics Institute, University College London, Gower Street, WC1E 6BT, London,
 69 UK
 70 ³² Non-profit Association Zirichiltaggi - Sardinia Wildlife Conservation, Strada Vicinale
 71 Filigheddu 62/C, I-07100 Sassari, Italy
 72 ³³ Laboratório de História Natural de Anfíbios Brasileiros (LaHNAB), Departamento de
 73 Biologia Animal, Instituto de Biologia, Unicamp, Campinas, Brazil
 74 ³⁴ ONG Ranita de Darwin, Nataniel Cox 152, Santiago, Chile
 75 ³⁵ Collection of Amphibians and Reptiles, Department of Zoology, Hungarian Natural
 76 History Museum, Budapest, Baross u. 13., 1088, Hungary
 77 ³⁶ Department of Ecology and Evolutionary Biology, Cornell University, Ithaca, NY, 14853,
 78 USA
 79 ³⁷ Centre for Genomic Pathogen Surveillance, Wellcome Genome Campus, Cambridgeshire,
 80 UK
 81 ³⁸ Museo Nacional de Ciencias Naturales, CSIC c/ Jose Gutierrez Abascal 2, 28006 Madrid,
 82 Spain
 83
 84 *Corresponding authors. Email: simon.ohanlon@gmail.com and
 85 matthew.fisher@imperial.ac.uk
 86
 87 †These authors share an equal contribution
 88

89 **One Sentence Summary:** East Asia is the source of amphibian panzootic chytrid fungi
90 causing global amphibian declines that have emerged during the 20th century
91

92 **Abstract:**

93 Globalized infectious diseases are causing species declines worldwide but their source often
94 remains elusive. We use whole-genome sequencing to solve the spatiotemporal origins of the
95 most devastating panzootic to date, caused by the fungus *Batrachochytrium dendrobatidis*, a
96 proximate driver of global amphibian declines. We trace the source of *B. dendrobatidis* to the
97 Korean peninsula where one lineage, *BdASIA-1*, exhibits the genetic hallmarks of an
98 ancestral population that seeded the panzootic. We date the emergence of this pathogen to the
99 early 20th century coinciding with the global expansion of commercial trade in amphibians
100 and show that intercontinental transmission is ongoing. Our findings point to East Asia as a
101 geographic hotspot for *B. dendrobatidis* biodiversity, and the original source of these lineages
102 that now parasitize amphibians worldwide.

103 Main Text:

104 Discovery of the amphibian-killing fungus *Batrachochytrium dendrobatidis* (1, 2) was a
105 turning point in understanding why amphibian species worldwide are in steep decline.
106 Amphibian declines and extinctions had been recorded by herpetologists as early as the
107 1970s, but were only recognized at a landmark meeting in 1990 as a global phenomenon
108 which could not be explained by environmental changes and anthropogenic factors alone (3).
109 The emergence of *B. dendrobatidis* and the disease that it causes, amphibian
110 chytridiomycosis, as a causative agent of declines has been documented across six different
111 regions: Australia (~1970s and 1990s) (4), Central America (~1970s) (5), South America
112 (~1970s and 1980s) (6, 7), the Caribbean islands (~2000s) (8), the North American Sierra
113 Nevada (~1980s and 1990s) (9), and the Iberian Peninsula (~1990s) (10). The panzootic has
114 been attributed to the emergence of a single *B. dendrobatidis* lineage, known as *BdGPL*
115 (Global Panzootic Lineage) (11). However, twenty years after identification of the disease,
116 the timing of its worldwide expansion remains unknown and previous estimates for time to
117 most recent common ancestor (TMRCA) for *BdGPL* span two orders of magnitude, from 100
118 ybp (11) to 26,000 ybp (12). The geographic origin of the pathogen is similarly contested,
119 with the source of the disease variously suggested to be Africa (13), North America (14),
120 South America (15), Japan (16) and East Asia (17).

121 Global diversity of *B. dendrobatidis*

122 To resolve these inconsistencies, we isolated *B. dendrobatidis* from all the candidate source
123 continents and sequenced the genomes of 177 isolates to high depth then combined our data
124 with published genomes from three prior studies (11, 12, 18) to generate a globally
125 representative panel of 234 isolates (Fig. 1A). This dataset covers all continents from which
126 *B. dendrobatidis* has been detected to date, and spans infections of all three extant orders of

127 Amphibia (Fig. S1 and Table S1). Mapped against the *B. dendrobatidis* reference genome
128 JEL423, our sequencing recovered 586,005 segregating single nucleotide polymorphisms
129 (SNPs). Phylogenetic analysis recovered all previously detected divergent lineages (Fig. 1B
130 and Fig. S2). The previously accepted lineages *BdGPL* (global), *BdCAPE* (African), *BdCH*
131 (European) and *BdBRAZIL* (Brazilian), were all detected (19), but our discovery of a new
132 hyperdiverse lineage in amphibians native to the Korean peninsula (*BdASIA-1*) redefined
133 these lineages and their relationships. The *BdCH* lineage, which was previously thought to be
134 enzootic to Switzerland (11) now groups with the *BdASIA-1* lineage. A second Asian-
135 associated lineage (*BdASIA-2*) was recovered from invasive North American bullfrogs in
136 Korea and is closely related to the lineage that is enzootic to the Brazilian Atlantic forest
137 (*BdBRAZIL*) (20). It was not possible to infer the direction of intercontinental spread
138 between isolates within this lineage so it was named *BdASIA-2/BdBRAZIL*. Conditional on
139 the midpoint rooting of the phylogeny in Fig. 1B, we now define the main diverged lineages
140 as *BdGPL*, *BdCAPE*, *BdASIA-1* (which includes the single *BdCH* isolate) and *BdASIA-*
141 *2/BdBRAZIL*. Previous phylogenetic relationships developed using the widely used
142 ribosomal intragenic spacer *ITS-1* region do not accurately distinguish *B. dendrobatidis*
143 lineages (Fig. S3) and this likely explains much of the place-of-origin conflict in the literature
144 (15-17).

145 Pairwise comparisons among isolates within each lineage show that the average number of
146 segregating sites is three-fold greater for *BdASIA-1* than for any other lineage (Fig. 1A and
147 Table 1) and that nucleotide diversity (π ; Fig. S4) is two to four-fold greater. Seven of our
148 eight *BdASIA-1* isolates were recently cultured from wild South Korean frogs while the other
149 came from the pet-trade in Belgium, all of which were aclinical infections. These isolates
150 show that the Korean peninsula is a global centre of *B. dendrobatidis* diversity and that East
151 Asia may contain the ancestral population of *B. dendrobatidis*, as suggested by Bataille *et al*

152 (17). We investigated this hypothesis further using Bayesian-based haplotype clustering (21)
153 and found the greatest haplotype sharing among isolates within *BdASIA-1* and between
154 *BdASIA-1* and all other lineages. This provides direct genetic evidence that *BdASIA-1* shares
155 more diversity with the global population of *B. dendrobatidis* than any other lineage (Fig.
156 S5). In an independent test of ancestry, we used OrthoMCL (22) to root a *B. dendrobatidis*
157 phylogeny to its closest known relative *B. salamandrivorans* which currently threatens
158 salamanders (23). This tree indicates that the Asian and Brazilian isolates of *B. dendrobatidis*
159 lie outside a clade comprising all other isolates (Fig. S6 and Table S2). To identify the
160 signature of demographic histories across lineages we used Tajima's *D* (24). Genome scans
161 of most lineages showed highly variable positive and negative values of *D* with maxima
162 exhibited by *BdGPL* (-2.6 to +6.2; Fig. 2F), indicating that these lineages (*BdASIA-*
163 *2/BdBRAZIL*, *BdCAPE* and *BdGPL*) have undergone episodes of population fluctuation,
164 strong natural selection, or both, that are consistent with a history of spatial and host
165 radiations. In striking contrast, *BdASIA-1* shows a flat profile for Tajima's *D* (Fig. 2F)
166 indicating mutation-drift equilibrium likely reflective of pathogen endemism in this region.

167 **Dating the emergence of *BdGPL***

168 The broad range of previous estimates for the TMRCA of *BdGPL* spanning 26,000 years (11,
169 12) can be explained by two sources of inaccuracy: (1) unaccounted recombination and (2)
170 the application of unrealistic evolutionary rates. To address these, we first interrogated the
171 178,280 kbp mitochondrial genome (mtDNA), which has high copy number and low rates of
172 recombination compared to the nuclear genome. To resolve the structure of the mtDNA
173 genome we resorted to long-read sequencing using a MinION device (Oxford Nanopore
174 Technologies, Cambridge, UK), which allowed us to describe this molecules unusual
175 configuration; *Batrachochytrium dendrobatidis* carries three linear mitochondrial segments,
176 each having inverted repeats at the termini with conserved mitochondrial genes spread over

177 two of the segments (Fig. S7). Additionally, we sought regions of the autosomal genome with
178 low rates of recombination to obtain an independent estimate of the TMRCA of *BdGPL*.

179 Detection of crossover events in the *B. dendrobatidis* autosomal genome (18) using a subset
180 of the isolates in this study revealed a large (1.66Mbp) region of Supercontig_1.2 in *BdGPL*
181 that exhibits several features that identified it as a recombination ‘coldspot’: (1) a continuous
182 region of reduced Tajima’s *D* (Fig. 2D); (2) sustained high values of F_{ST} when compared
183 with all other lineages (Fig. 3A); (3) a continuous region of reduced nucleotide diversity (π ,
184 Fig. S4) and (4) shared loss-of-heterozygosity (Fig. S8). We expanded sampling to infer the
185 temporal range of pathogen introductions using a broad panel of isolates with known date of
186 isolation ($n = 184$, ranging from 1998 to 2016) and whole-genome RNA-baiting to obtain
187 reads from preserved amphibians that had died of chytridiomycosis. We then investigated
188 whether our dataset contained sufficient signal to perform tip-dating inferences by building
189 phylogenetic trees using PhyML (25) (Fig. 2A and 2C) then fitting root-to-tip distances to
190 collection dates both at the whole-tree and within-lineage scales. We observed a positive and
191 significant correlation within *BdGPL* only, for both the mitochondrial and nuclear genomes,
192 demonstrating sufficient temporal signal to perform thorough tip-dating inferences at this
193 evolutionary scale (Fig. 2B and 2D).

194 Tip-dating in BEAST was used to co-estimate ancestral divergence times and the rate at
195 which mutations accumulate within the *BdGPL* lineage. The mean mitochondrial substitution
196 rate was 1.01×10^{-6} substitutions/site/year (95% highest posterior density (HPD) $4.29 \times 10^{-7} -$
197 1.62×10^{-6}). The mean nuclear substitution rate was 7.29×10^{-7} substitutions/site/year (95%
198 HPD $3.41 \times 10^{-7} - 1.14 \times 10^{-6}$), which is comparable to a recent report of an evolutionary rate
199 of $2.4 - 2.6 \times 10^{-6}$ substitutions/site/year for another unicellular yeast, *Saccharomyces*
200 *cerevisiae* beer strains (26). These estimates are over 300-fold faster than the rate used in a

201 previous study (12) to obtain a TMRCA of 26,400 years for *BdGPL*. Accordingly, we
202 estimate the ancestor of the amphibian panzootic *BdGPL* originated between 120 and 50
203 years ago (Fig. 2E), with HPD estimates of 1898 [95% HPD 1809-1941] and 1962 [95%
204 HPD 1859-1988] for the nuclear and mitochondrial dating analyses respectively (Fig. 2F).

205 We considered an additional calibration approach for the TMRCA of the mitochondrial
206 genome where we included informative priors on nodes around the dates for the first
207 historical descriptions of *BdGPL* detection in Australia (1978), Central America (1972),
208 Sierra de Guadarrama (Europe) (1997), and the Pyrenees (Europe) (2000). We did not
209 include priors for nodes where observed declines have been reported, but where the lineage
210 responsible for those declines is unknown. This mixed dating method based on tips and nodes
211 calibration yielded very similar estimates (TMRCA estimates of 1975 [95% HPD 1939 –
212 1989] (Fig. S9)), further strengthening our confidence in a recent date of emergence for
213 *BdGPL*. An expansion of *BdGPL* in the 20th century coincides with the global expansion in
214 amphibians traded for exotic pets, medical and food purposes (27, 28). Within our phylogeny,
215 we found representatives from all lineages among traded animals (Figs. S10-14), and
216 identified ten events where traded amphibians were infected with non-enzootic isolates (Fig.
217 4). This finding demonstrates the ongoing failure of international biosecurity despite the
218 listing of *B. dendrobatidis* by the World Organisation for Animal Health (the OIE) in 2008.

219 **Hybridisation between recontacting lineages of *B. dendrobatidis***

220 To determine the extent to which the four main lineages of *B. dendrobatidis* have undergone
221 recent genetic exchange, we used the site-by-site based approach implemented in
222 STRUCTURE (29). Although most isolates could be assigned unambiguously to one of the
223 four main lineages, we identified three hybrid genotypes (Fig. 3B), including one previously
224 reported hybrid (isolate CLFT024/2) (20), and discovered two newly identified hybrids of

225 *BdGPL* and *BdCAPE* in South Africa. Furthermore, *BdCH* (isolate 0739) appears to be a
226 chimera of multiple lineages that may represent unsampled genomic diversity that resides in
227 East Asia, rather than true hybridisation. These hybrid genomes demonstrate that *B.*
228 *dendrobatidis* is continuing to exchange haplotypes among lineages when they interact
229 following continental invasions, generating novel genomic diversity. We analysed isolate
230 clustering using principle components analysis on a filtered subset of 3,900 SNPs in linkage
231 equilibrium, revealing an overall population structure that is consistent with our phylogenetic
232 analyses (Fig 3C). In addition, the putatively identified hybrid isolates of *B. dendrobatidis*
233 were shown to fall between main lineage clusters (Fig. 3C) further strengthening our
234 hypothesis of haplotype exchange occurring during secondary contact between lineages.

235 **Associations among lineage, virulence and declines**

236 Genotypic diversification of pathogens is commonly associated with diversification of traits
237 associated with host exploitation (30), and is most commonly measured as the ability to infect
238 a host and to cause disease post-infection. We tested for variation of these two phenotypic
239 traits across four *B. dendrobatidis* lineages by exposing larval and post-metamorphic
240 common toads (*Bufo bufo*). Larvae are highly susceptible to infection but do not die before
241 metamorphosis, in contrast to post-metamorphic juveniles, which are susceptible to infection
242 and fatal chytridiomycosis (31). In tadpoles, both *BdGPL* and *BdASIA-1* were significantly
243 more infectious than *BdCAPE* and *BdCH* (Fig. S15 and Tables S3 & S4). In metamorphs,
244 *BdGPL* was significantly more infectious than the other treatments, compared to the control
245 group, and significantly more lethal in experimental challenge, than the geographically more
246 restricted *BdCAPE*, *BdASIA-1* and *BdCH* (Fig. 2G). We further tested for differences in
247 virulence among lineages by using our global dataset to examine whether chytridiomycosis
248 was non-randomly associated with *B. dendrobatidis* lineage. We detected a significant

249 difference ($p < 0.001$) in the proportion of isolates associated with chytridiomycosis among
250 the three parental lineages (*BdASIA-1* and *BdASIA-2/BdBRAZIL* were grouped due to low
251 sample sizes), and *post hoc* tests indicated significant excess in virulence in both *BdGPL* and
252 *BdCAPE* lineages relative to the combined *BdASIA-1* and *BdASIA-2/BdBRAZIL* (all $p <$
253 0.05). However, we did not detect a significant difference between *BdGPL* and *BdCAPE*
254 (Fig. S16 and Table S5). These data suggest that although *BdGPL* is highly virulent,
255 population-level outcomes are also context dependent (32); under some conditions other
256 lineages can also be responsible for lethal amphibian disease and population declines (33).

257 **Historical and contemporary implications of panzootic chytridiomycosis**

258 Our results point to endemism of *B. dendrobatidis* in Asia, out of which multiple panzootic
259 lineages have emerged. These emergent diasporas include the virulent and highly
260 transmissible *BdGPL* which spread during the early 20th century via a yet unknown route to
261 infect close to 700 amphibian species out of ~1300 thus far tested (34). With over 7800
262 amphibian species currently described, the number of affected species is likely to rise. The
263 international trade in amphibians has undoubtedly contributed directly to vectoring this
264 pathogen worldwide (Fig. 4; 35,36), and within our phylogeny we identified many highly
265 supported ($\geq 90\%$ bootstrap support) clades on short branches that linked isolates collected
266 from wild amphibian populations across different continents (Fig. 4; Fig. S10-S14).
267 However, the role of globalised trade in passively contributing to the spread of this disease
268 cannot be ruled out. It is likely no coincidence that our estimated dates for the emergence of
269 *BdGPL* span the globalisation ‘big bang’, the rapid proliferation in intercontinental trade,
270 capital, and technology that started in the 1820s (37). The recent invasion of Madagascar by
271 Asian common toads hidden within mining equipment (38) demonstrates the capacity for
272 amphibians to escape detection at borders and exemplifies how the unintended anthropogenic

273 dispersal of amphibians has also likely contributed to the worldwide spread of pathogenic
274 chytrids.

275 The hyperdiverse hotspot identified in Korea likely represents a fraction of the
276 *Batrachochytrium* genetic diversity in Asia and further sampling across this region is
277 urgently needed because the substantial global trade in Asian amphibians (39) presents a risk
278 of seeding future outbreak lineages. Unique ribosomal DNA haplotypes of *B. dendrobatidis*
279 have been detected in native amphibian species in India (40, 41), Japan (16) and China (42).
280 Although caution should be observed when drawing conclusions about lineages based on
281 short sequence alignments (Fig. S3), other endemic lineages probably remain undetected
282 within Asia. Significantly, the northern European countryside is witnessing the emergence of
283 *B. salamandrivorans*, which also has its origin in Asia. The emergence of *B.*
284 *salamandrivorans* is linked to the amphibian pet trade (43), and the broad expansion of
285 virulence factors that are found in the genomes of these two pathogens are testament to the
286 evolutionary innovation that has occurred in these Asian *Batrachochytrium* fungi (23). Our
287 findings show that the global trade in amphibians continues to be associated with the
288 translocation of chytrid lineages with panzootic potential. Ultimately, our work confirms that
289 panzootics of emerging fungal diseases in amphibians are caused by ancient patterns of
290 pathogen phylogeography being redrawn as largely unrestricted global trade moves
291 pathogens into new regions, infecting new hosts and igniting disease outbreaks. Within this
292 context, the continued strengthening of transcontinental biosecurity is critical to the survival
293 of amphibian species in the wild (44).

294 **References:**

- 295 1. M. C. Fisher, D. A. Henk, C. J. Briggs, J. S. Brownstein, L. C. Madoff, S. L. McCraw, S. J.
296 Gurr, Emerging fungal threats to animal, plant and ecosystem health. *Nature* **484**, 186-194
297 (2012).
- 298 2. L. Berger, R. Speare, P. Daszak, D. E. Green, A. A. Cunningham, C. L. Goggin, R.
299 Slocombe, M. A. Ragan, A. H. Hyatt, K. R. McDonald, H. B. Hines, K. R. Lips, G.
300 Marantelli, H. Parkes, Chytridiomycosis causes amphibian mortality associated with
301 population declines in the rain forests of Australia and Central America. *P Natl Acad Sci USA*
302 **95**, 9031-9036 (1998).
- 303 3. A. R. Blaustein, D. B. Wake, Declining amphibian populations: A global phenomenon?
304 *Trends Ecol Evol* **5**, 203-204 (1990).
- 305 4. L. F. Skerratt, L. Berger, R. Speare, S. Cashins, K. R. McDonald, A. D. Phillott, H. B. Hines,
306 N. Kenyon, Spread of chytridiomycosis has caused the rapid global decline and extinction of
307 frogs. *Ecohealth* **4**, 125-134 (2007).
- 308 5. T. L. Cheng, S. M. Rovito, D. B. Wake, V. T. Vredenburg, Coincident mass extirpation of
309 neotropical amphibians with the emergence of the infectious fungal pathogen
310 *Batrachochytrium dendrobatidis*. *P Natl Acad Sci USA* **108**, 9502-9507 (2011).
- 311 6. K. R. Lips, J. Diffendorfer, J. R. Mendelson, M. W. Sears, Riding the wave: Reconciling the
312 roles of disease and climate change in amphibian declines. *Plos Biol* **6**, 441-454 (2008).
- 313 7. T. Carvalho, C. G. Becker, L. F. Toledo, Historical amphibian declines and extinctions in
314 Brazil linked to chytridiomycosis. *Proc Royal Soc B* **284**, 20162254 (2017).
- 315 8. M. A. Hudson, R. P. Young, J. D. Jackson, P. Orozco-terWengel, L. Martin, A. James, M.
316 Sulton, G. Garcia, R. A. Griffiths, R. Thomas, C. Magin, M. W. Bruford, A. A. Cunningham,
317 Dynamics and genetics of a disease-driven species decline to near extinction: lessons for
318 conservation. *Sci Rep* **6**, srep30772 (2016).

- 319 9. L. J. Rachowicz, R. A. Knapp, J. A. T. Morgan, M. J. Stice, V. T. Vredenburg, J. M. Parker,
320 C. J. Briggs, Emerging infectious disease as a proximate cause of amphibian mass mortality.
321 *Ecology* **87**, 1671-1683 (2006).
- 322 10. J. Bosch, I. Martinez-Solano, M. Garcia-Paris, Evidence of a chytrid fungus infection
323 involved in the decline of the common midwife toad (*Alytes obstetricans*) in protected areas
324 of central Spain. *Biol Conserv* **97**, 331-337 (2001).
- 325 11. R. A. Farrer, L. A. Weinert, J. Bielby, T. W. J. Garner, F. Balloux, F. Clare, J. Bosch, A. A.
326 Cunningham, C. Weldon, L. H. du Preez, L. Anderson, S. L. K. Pond, R. Shahar-Golan, D. A.
327 Henk, M. C. Fisher, Multiple emergences of genetically diverse amphibian-infecting chytrids
328 include a globalized hypervirulent recombinant lineage. *P Natl Acad Sci USA* **108**, 18732-
329 18736 (2011).
- 330 12. E. B. Rosenblum, T. Y. James, K. R. Zamudio, T. J. Poorten, D. Ilut, D. Rodriguez, J. M.
331 Eastman, K. Richards-Hrdlicka, S. Joneson, T. S. Jenkinson, J. E. Longcore, G. P. Olea, L. F.
332 Toledo, M. L. Arellano, E. M. Medina, S. Restrepo, S. V. Flechas, L. Berger, C. J. Briggs, J.
333 E. Stajich, Complex history of the amphibian-killing chytrid fungus revealed with genome
334 resequencing data. *P Natl Acad Sci USA* **110**, 9385-9390 (2013).
- 335 13. C. Weldon, L. H. du Preez, A. D. Hyatt, R. Muller, R. Speare, Origin of the amphibian
336 chytrid fungus. *Emerg Infect Dis* **10**, 2100-2105 (2004).
- 337 14. B. L. Talley, C. R. Muletz, V. T. Vredenburg, R. C. Fleischer, K. R. Lips, A century of
338 *Batrachochytrium dendrobatidis* in Illinois amphibians (1888-1989). *Biol Conserv* **182**, 254-
339 261 (2015).
- 340 15. D. Rodriguez, C. G. Becker, N. C. Pupin, C. F. B. Haddad, K. R. Zamudio, Long-term
341 endemism of two highly divergent lineages of the amphibian-killing fungus in the Atlantic
342 Forest of Brazil. *Mol Ecol* **23**, 774-787 (2014).
- 343 16. K. Goka, J. Yokoyama, Y. Une, T. Kuroki, K. Suzuki, M. Nakahara, A. Kobayashi, S. Inaba,
344 T. Mizutani, A. D. Hyatt, Amphibian chytridiomycosis in Japan: distribution, haplotypes and
345 possible route of entry into Japan. *Mol Ecol* **18**, 4757-4774 (2009).

- 346 17. A. Bataille, J. J. Fong, M. Cha, G. O. U. Wogan, H. J. Baek, H. Lee, M. S. Min, B. Waldman,
347 Genetic evidence for a high diversity and wide distribution of endemic strains of the
348 pathogenic chytrid fungus *Batrachochytrium dendrobatidis* in wild Asian amphibians. *Mol*
349 *Ecol* **22**, 4196-4209 (2013).
- 350 18. R. A. Farrer, D. A. Henk, T. W. J. Garner, F. Balloux, D. C. Woodhams, M. C. Fisher,
351 Chromosomal copy number variation, selection and uneven rates of recombination reveal
352 cryptic genome diversity linked to pathogenicity. *Plos Genet* **9**, e1003703 (2013).
- 353 19. S. Argimón, K. Abudahab, R. J. E. Goater, A. Fedosejev, J. Bhai, C. Glasner, E. J. Feil, M. T.
354 G. Holden, C. A. Yeats, H. Grundmann, B. G. Spratt, D. M. Aanensen, Microreact:
355 visualizing and sharing data for genomic epidemiology and phylogeography. *Microbial*
356 *Genomics* **2**, e000093 (2016).
- 357 20. L. M. Schloegel, L. F. Toledo, J. E. Longcore, S. E. Greenspan, C. A. Vieira, M. Lee, S.
358 Zhao, C. Wangen, C. M. Ferreira, M. Hipolito, A. J. Davies, C. A. Cuomo, P. Daszak, T. Y.
359 James, Novel, panzootic and hybrid genotypes of amphibian chytridiomycosis associated with
360 the bullfrog trade. *Mol Ecol* **21**, 5162-5177 (2012).
- 361 21. D. J. Lawson, G. Hellenthal, S. Myers, D. Falush, Inference of population structure using
362 dense haplotype data. *Plos Genet* **8**, e1002453 (2012).
- 363 22. L. Li, C. J. Stoeckert, Jr., D. S. Roos, OrthoMCL: identification of ortholog groups for
364 eukaryotic genomes. *Genome Res* **13**, 2178-2189 (2003).
- 365 23. R. A. Farrer, A. Martel, E. Verbrugghe, A. Abouelleil, R. Ducatelle, J. E. Longcore, T. Y.
366 James, F. Pasmans, M. C. Fisher, C. A. Cuomo, Genomic innovations linked to infection
367 strategies across emerging pathogenic chytrid fungi. *Nat Commun* **8**, 14742 (2017).
- 368 24. F. Tajima, Statistical-Method for Testing the Neutral Mutation Hypothesis by DNA
369 Polymorphism. *Genetics* **123**, 585-595 (1989).
- 370 25. S. Guindon, J. F. Dufayard, V. Lefort, M. Anisimova, W. Hordijk, O. Gascuel, New
371 algorithms and methods to estimate maximum-likelihood phylogenies: assessing the
372 performance of PhyML 3.0. *Syst Biol* **59**, 307-321 (2010).

- 373 26. B. Gallone, J. Steensels, T. Prah, L. Soriaga, V. Saels, B. Herrera-Malaver, A. Merlevede, M.
374 Roncoroni, K. Voordeckers, L. Miraglia, C. Teiling, B. Steffy, M. Taylor, A. Schwartz, T.
375 Richardson, C. White, G. Baele, S. Maere, K. J. Verstrepen, Domestication and divergence of
376 *Saccharomyces cerevisiae* beer yeasts. *Cell* **166**, 1397-1410.e16 (2016).
- 377 27. M. C. Fisher, T. W. J. Garner, The relationship between the emergence of *Batrachochytrium*
378 *dendrobatidis*, the international trade in amphibians and introduced amphibian species.
379 *Fungal Biol Rev* **21**, 2-9 (2007).
- 380 28. A. I. Carpenter, F. Andreone, R. D. Moore, R. A. Griffiths, A review of the international trade
381 in amphibians: the types, levels and dynamics of trade in CITES-listed species. *Oryx* **48**, 565-
382 574 (2014).
- 383 29. J. K. Pritchard, M. Stephens, P. Donnelly, Inference of population structure using multilocus
384 genotype data. *Genetics* **155**, 945-959 (2000).
- 385 30. S. J. Price, T. W. Garner, R. A. Nichols, F. Balloux, C. Ayres, A. Mora-Cabello de Alba, J.
386 Bosch, Collapse of amphibian communities due to an introduced ranavirus. *Curr Biol* **24**,
387 2586-2591 (2014).
- 388 31. T. W. J. Garner, S. Walker, J. Bosch, S. Leech, J. M. Rowcliffe, A. A. Cunningham, M. C.
389 Fisher, Life history tradeoffs influence mortality associated with the amphibian pathogen
390 *Batrachochytrium dendrobatidis*. *Oikos* **118**, 783-791 (2009).
- 391 32. K. A. Bates, F. C. Clare, S. O'Hanlon, J. Bosch, L. Brookes, K. Hopkins, E. J. McLaughlin,
392 O. Daniel, T. W. J. Garner, M. C. Fisher, X. A. Harrison, Amphibian chytridiomycosis
393 outbreak dynamics are linked with host skin bacterial community structure. *Nat Commun* **9**,
394 693 (2018).
- 395 33. B. J. Doddington, J. Bosch, J. A. Oliver, N. C. Grassly, G. Garcia, B. R. Schmidt, T. W.
396 Garner, M. C. Fisher, Context-dependent amphibian host population response to an invading
397 pathogen. *Ecology* **94**, 1795-1804 (2013).
- 398 34. D. H. Olson, K. L. Ronnenberg, Global Bd Mapping Project: 2014 Update. *FrogLog*, 22, p17-
399 21 (2014).

- 400 35. S. F. Walker, J. Bosch, T. Y. James, A. P. Litvintseva, J. A. O. Valls, S. Piña, G. García, G.
401 A. Rosa, A. A. Cunningham, S. Hole, R. Griffiths, M. C. Fisher, Invasive pathogens threaten
402 species recovery programs, *Curr Biol* **18**, R853-R854 (2008).
- 403 36. E. L. Wombwell, T. W. J. Garner, A. A. Cunningham, R. Quest, S. Pritchard, J. M.
404 Rowcliffe, R. Griffiths, Detection of *Batrachochytrium dendrobatidis* in amphibians imported
405 into the UK for the pet trade. *EcoHealth* **13**, 456-466 (2016).
- 406 37. K. H. O'Rourke, J. G. Williamson, When did globalisation begin? *Eur Rev Econ Hist* **6**, 23–
407 50 (2002).
- 408 38. J. E. Kolby, Ecology: Stop Madagascar's toad invasion now, *Nature* **509**, 563 (2014).
- 409 39. A. Herrel, A. van der Meijden, An analysis of the live reptile and amphibian trade in the USA
410 compared to the global trade in endangered species. *Herpetol J* **24**, 103-110 (2014).
- 411 40. N. Dahanukar, K. Krutha, M. S. Paingankar, A. D. Padhye, N. Modak, S. Molur, Endemic
412 Asian chytrid strain infection in threatened and endemic anurans of the northern Western
413 Ghats, India. *PLoS One* **8**, e77528 (2013)
- 414 41. S. Molur, K. Krutha, M.S. Paingankar, N. Dahanukar, Asian strain of *Batrachochytrium*
415 *dendrobatidis* is widespread in the Western Ghats, India. *Dis Aquat Organ* **112**, 251-255
416 (2015).
- 417 42. C. Bai, X. Liu, M. C. Fisher, W. J. T. Garner, Y. Li, Global and endemic Asian lineages of
418 the emerging pathogenic fungus *Batrachochytrium dendrobatidis* widely infect amphibians in
419 China. *Divers Distrib* **18**, 307-318 (2012).
- 420 43. A. Martel, M. Blooi, C. Adriaensen, P. Van Rooij, W. Beukema, M. C. Fisher, R. A. Farrer,
421 B. R. Schmidt, U. Tobler, K. Goka, K. R. Lips, C. Muletz, K. R. Zamudio, J. Bosch, S.
422 Lotters, E. Wombwell, T. W. Garner, A. A. Cunningham, A. Spitzen-van der Sluijs, S.
423 Salvidio, R. Ducatelle, K. Nishikawa, T. T. Nguyen, J. E. Kolby, I. Van Bocxlaer, F. Bossuyt,
424 F. Pasmans, Wildlife disease. Recent introduction of a chytrid fungus endangers Western
425 Palearctic salamanders. *Science* **346**, 630-631 (2014).
- 426 44. H. E. Roy, H. Hesketh, B. V. Purse, J. Eilenberg, A. Santini, R. Scalera, G. D. Stentiford, T.
427 Adriaens, K. Bacela-Spychalska, D. Bass, K. M. Beckmann, P. Bessell, J. Bojko, O. Booy, A.

- 428 C. Cardoso, F. Essl, Q. Groom, C. Harrower, R. Kleespies, A. F. Martinou, M. M. van Oers,
429 E. J. Peeler, J. Pergl, W. Rabitsch, A. Roques, F. Schaffner, S. Schindler, B. R. Schmidt, K.
430 Schonrogge, J. Smith, W. Solarz, A. Stewart, A. Stroo, E. Tricarico, K. M. A. Turvey, A.
431 Vannini, M. Vila, S. Woodward, A. A. Wynns, A. M. Dunn, Alien pathogens on the horizon:
432 opportunities for predicting their threat to wildlife. *Conserv Lett* **10**, 477-484 (2017).
- 433 45. M. Martin, Cutadapt removes adapter sequences from high-throughput sequencing reads.
434 *EMBnet. journal* **17**, 10-12 (2011).
- 435 46. H. Li, Aligning sequence reads, clone sequences and assembly contigs with BWA-MEM.
436 *arXiv preprint arXiv:1303.3997*, (2013).
- 437 47. H. Li, B. Handsaker, A. Wysoker, T. Fennell, J. Ruan, N. Homer, G. Marth, G. Abecasis, R.
438 Durbin, The sequence alignment/map format and SAMtools. *Bioinformatics* **25**, 2078-2079
439 (2009).
- 440 48. E. Garrison, G. Marth, Haplotype-based variant detection from short-read sequencing. *arXiv*
441 *preprint arXiv:1207.3907*, (2012).
- 442 49. E. Garrison, Vcfliib: A C++ library for parsing and manipulating VCF files. *GitHub*
443 <https://github.com/ekg/vcfliib> (accessed July 21, 2015), (2012).
- 444 50. A. Tan, G. R. Abecasis, H. M. Kang, Unified representation of genetic variants.
445 *Bioinformatics* **31**, 2202-2204 (2015).
- 446 51. A. Stamatakis, RAxML version 8: a tool for phylogenetic analysis and post-analysis of large
447 phylogenies. *Bioinformatics* **30**, 1312-1313 (2014).
- 448 52. A. McKenna, M. Hanna, E. Banks, A. Sivachenko, K. Cibulskis, A. Kernytzsky, K. Garimella,
449 D. Altshuler, S. Gabriel, M. Daly, The Genome Analysis Toolkit: a MapReduce framework
450 for analyzing next-generation DNA sequencing data. *Genome Res* **20**, 1297-1303 (2010).
- 451 53. S. Guindon, J. F. Dufayard, V. Lefort, M. Anisimova, W. Hordijk, O. Gascuel, New
452 algorithms and methods to estimate maximum-likelihood phylogenies: assessing the
453 performance of PhyML 3.0. *Syst Biol* **59**, 307-321 (2010).
- 454 54. A. J. Drummond, M. A. Suchard, D. Xie, A. Rambaut, Bayesian phylogenetics with BEAUti
455 and the BEAST 1.7. *Mol Biol Evol* **29**, 1969-1973 (2012).

- 456 55. D. Posada, K. A. Crandall, MODELTEST: testing the model of DNA substitution.
457 *Bioinformatics* **14**, 817-818 (1998).
- 458 56. A. Rieux, F. Balloux, Inferences from tip-calibrated phylogenies: a review and a practical
459 guide. *Mol Ecol*, **25**, 1911-1924 (2016).
- 460 57. S. F. Walker, J. Bosch, V. Gomez, T. W. Garner, A. A. Cunningham, D. S. Schmeller, M.
461 Ninyerola, D. A. Henk, C. Ginestet, C. P. Arthur, M. C. Fisher, Factors driving pathogenicity
462 vs. prevalence of amphibian panzootic chytridiomycosis in Iberia. *Ecol Lett* **13**, 372-382
463 (2010).
- 464 58. N. Wales, C. Caroe, M. Sandoval-Velasco, C. Gamba, R. Barnett, J. A. Samaniego, J. R.
465 Madrigal, L. Orlando, M. T. Gilbert, New insights on single-stranded versus double-stranded
466 DNA library preparation for ancient DNA. *BioTechniques* **59**, 368-371 (2015).
- 467 59. M. Schubert, L. Ermini, C. Der Sarkissian, H. Jonsson, A. Ginolhac, R. Schaefer, M. D.
468 Martin, R. Fernandez, M. Kircher, M. McCue, E. Willerslev, L. Orlando, Characterization of
469 ancient and modern genomes by SNP detection and phylogenomic and metagenomic analysis
470 using PALEOMIX. *Nat Protoc* **9**, 1056-1082 (2014).
- 471 60. S. Koren, B. P. Walenz, K. Berlin, J. R. Miller, N. H. Bergman, A. M. Phillippy, Canu:
472 scalable and accurate long-read assembly via adaptive k-mer weighting and repeat separation.
473 *Genome Res* **27**, 722-736 (2017).
- 474 61. I. Sovic, M. Sikic, A. Wilm, S. N. Fenlon, S. Chen, N. Nagarajan, Fast and sensitive mapping
475 of nanopore sequencing reads with GraphMap. *Nat Commun* **7**, 11307 (2016).
- 476 62. B. J. Walker, T. Abeel, T. Shea, M. Priest, A. Abouelliel, S. Sakthikumar, C. A. Cuomo, Q.
477 Zeng, J. Wortman, S. K. Young, A. M. Earl, Pilon: an integrated tool for comprehensive
478 microbial variant detection and genome assembly improvement. *PLoS One* **9**, e112963
479 (2014).
- 480 63. N. Beck, B. Lang, MFannot. *MFannot Tool* Available at:
481 <http://megasun.bch.umontreal.ca/cgi-bin/mfannot/mfannotInterface.pl>. (Accessed: 28th
482 January 2018)

- 483 64. P. Jones, D. Binns, H. Y. Chang, M. Fraser, W. Li, C. McAnulla, H. McWilliam, J. Maslen,
484 A. Mitchell, G. Nuka, S. Pesseat, A. F. Quinn, A. Sangrador-Vegas, M. Scheremetjew, S. Y.
485 Yong, R. Lopez, S. Hunter, InterProScan 5: genome-scale protein function classification.
486 *Bioinformatics* **30**, 1236-1240 (2014).
- 487 65. T. M. Lowe, P. P. Chan, tRNAscan-SE On-Line: Integrating Search and Context for Analysis
488 of Transfer RNA Genes. *Nucleic Acids Res*, **44**, W54–W57 (2016).
- 489 66. T. M. Lowe, S. R. Eddy, tRNAscan-SE: a program for improved detection of transfer RNA
490 genes in genomic sequence. *Nucleic Acids Res* **25**, 955-964 (1997).
- 491 67. P. Danecek, A. Auton, G. Abecasis, C. A. Albers, E. Banks, M. A. DePristo, R. E. Handsaker,
492 G. Lunter, G. T. Marth, S. T. Sherry, The variant call format and VCFtools. *Bioinformatics*
493 **27**, 2156-2158 (2011).
- 494 68. D. J. Lawson, G. Hellenthal, S. Myers, D. Falush, Inference of population structure using
495 dense haplotype data. *Plos Genet* **8**, e1002453 (2012).
- 496 69. O. Delaneau, B. Howie, A. J. Cox, J. F. Zagury, J. Marchini, Haplotype Estimation using
497 sequencing reads. *Am J Hum Genet* **93**, 687-696 (2013).
- 498 70. D. Falush, M. Stephens, J. K. Pritchard, Inference of population structure using multilocus
499 genotype data: Linked loci and correlated allele frequencies. *Genetics* **164**, 1567-1587 (2003).
- 500 71. G. Evanno, S. Regnaut, J. Goudet, Detecting the number of clusters of individuals using the
501 software STRUCTURE: a simulation study. *Mol Ecol* **14**, 2611-2620 (2005).
- 502 72. X. Zheng, D. Levine, J. Shen, S. M. Gogarten, C. Laurie, B. S. Weir, A high-performance
503 computing toolset for relatedness and principal component analysis of SNP data.
504 *Bioinformatics* **28**, 3326-3328 (2012).
- 505 73. R Core Team. (R Foundation for Statistical Computing, Vienna, Austria, 2017).
- 506 74. H. Wickham, *ggplot2 : elegant graphics for data analysis*. Use R! (Springer, New York,
507 2009), pp. viii, 212 p.
- 508 75. K. L. Gosner, A simplified table for staging anuran embryos and larvae with notes on
509 identification. *Herpetologica* **16**, 183-190 (1960).

- 510 76. D. G. Boyle, D. B. Boyle, V. Olsen, J. A. Morgan, A. D. Hyatt, Rapid quantitative detection
511 of chytridiomycosis (*Batrachochytrium dendrobatidis*) in amphibian samples using real-time
512 Taqman PCR assay. *Dis Aquat Organ* **60**, 141-148 (2004).
- 513 77. K. M. Kriger, H. B. Hines, A. D. Hyatt, D. G. Boyle, J. M. Hero, Techniques for detecting
514 chytridiomycosis in wild frogs: comparing histology with real-time Taqman PCR. *Dis Aquat*
515 *Organ* **71**, 141-148 (2006).
- 516 78. P. Kleinhenz, M. D. Boone, G. Fellers, Effects of the amphibian chytrid fungus and four
517 insecticides on Pacific treefrogs (*Pseudacris regilla*). *J Herpetol* **46**, 625-631 (2012).
- 518 79. E. Luquet, T. W. Garner, J. P. Lena, C. Bruel, P. Joly, T. Lengagne, O. Grolet, S. Plenet,
519 Genetic erosion in wild populations makes resistance to a pathogen more costly. *Evolution*
520 **66**, 1942-1952 (2012).
- 521 80. M. J. Parris, T. O. Cornelius, Fungal pathogen causes competitive and developmental stress in
522 larval amphibian communities. *Ecology* **85**, 3385-3395 (2004).
- 523 81. D. Darriba, G. L. Taboada, R. Doallo, D. Posada, ProtTest 3: fast selection of best-fit models
524 of protein evolution. *Bioinformatics* **27**, 1164-1165 (2011).
- 525 82. K. Tamura, G. Stecher, D. Peterson, A. Filipinski, S. Kumar, MEGA6: Molecular Evolutionary
526 Genetics Analysis Version 6.0. *Mol Biol Evol* **30**, 2725-2729 (2013).
- 527 83. R. R. Wick, M. B. Schultz, J. Zobel, K. E. Holt, Bandage: interactive visualization of de novo
528 genome assemblies. *Bioinformatics* **31**, 3350-3352 (2015).
- 529 84. M. J. Laforest, I. Roewer, B. F. Lang, Mitochondrial tRNAs in the lower fungus
530 *Spizellomyces punctatus*: tRNA editing and UAG 'stop' codons recognized as leucine. *Nucleic*
531 *Acids Res* **25**, 626-632 (1997).
- 532 85. E. Kayal, B. Bintlage, A. G. Collins, M. Kayal, S. Pirro, D. V. Lavrov, Evolution of linear
533 mitochondrial genomes in medusozoan cnidarians. *Genome Biol Evol* **4**, 1-12 (2012).
- 534 86. Z. Shao, S. Graf, O. Y. Chaga, D. V. Lavrov, Mitochondrial genome of the moon jelly
535 *Aurelia aurita* (Cnidaria, Scyphozoa): A linear DNA molecule encoding a putative DNA-
536 dependent DNA polymerase. *Gene* **381**, 92-101 (2006).

- 537 87. M. Valach, Z. Farkas, D. Fricova, J. Kovac, B. Brejova, T. Vinar, I. Pfeiffer, J. Kucsera, L.
 538 Tomaska, B. F. Lang, J. Nosek, Evolution of linear chromosomes and multipartite genomes in
 539 yeast mitochondria. *Nucleic Acids Res* **39**, 4202-4219 (2011).
- 540 88. C. A. Brewer, <http://www.ColorBrewer.org> (2018).
- 541 89. E. Neuwirth, RColorBrewer: ColorBrewer Palettes. R package version 1.1-2.
 542 <https://CRAN.R-project.org/package=RColorBrewer> (2014).
- 543 90. M. Dowle, A. Srinivasan, data.table: Extension of `data.frame`. R package version 1.10.4.
 544 <https://CRAN.R-project.org/package=data.table> (2017).
- 545 91. G. Yu, D. Smith, H. Zhu, Y. Guan, T. T-Y. Lam, ggtree: an R package for visualization and
 546 annotation of phylogenetic trees with their covariates and other associated data. *Meth Ecol*
 547 *Evol* **8**, 28-36 (2017).
- 548 92. T. Galili, dendextend: an R package for visualizing, adjusting, and comparing trees of
 549 hierarchical clustering. *Bioinformatics* **31**, 3718-3720 (2015).

550

551 **Acknowledgments:**

552 DNA sequencing was carried out in the NBAF GenePool genomics facility at the University
 553 of Edinburgh, and we thank the GenePool staff for their assistance. This work used the
 554 computing resources of the UK MEDical BIOinformatics partnership - aggregation,
 555 integration, visualisation and analysis of large, complex data (UK MED-BIO) which is
 556 supported by the Medical Research Council [grant number MR/L01632X/1]. We thank Dr
 557 Johanna Rhodes for the provision of flow cells and reagents for MinION sequencing. We
 558 thank the staff at Oxford Nanopore Technologies for admission to the MinION Early Access
 559 Programme. We thank the three anonymous reviewers for constructive comments and
 560 suggestions during the peer review process.

561 **Funding:** SOH, TWJG, LB (Brookes), AL, AAC, DSS, EC, CM, JB, DA, FC and MCF were
 562 supported through NERC (standard grant NE/K014455/1). SOH acknowledges a Microsoft

563 Azure for Research Sponsorship (subscription ID: ab7cd695-49cf-4a83-910a-ef71603e708b).
564 TWJG, AL, AAC, DSS, EC, CM, JB, DA, FC and MCF were also supported by the EU
565 BiodivERsA scheme (R.A.C.E., funded through NERC directed grant NE/ G002193/1 and
566 ANR-08-Biodiversa-002-03) and NERC (standard grant NE/K012509/1). MCF, EC and CM
567 acknowledge the Nouragues Travel Grant Program 2014. RAF was supported by an MIT /
568 Wellcome Trust Fellowship. TWJG was supported by the People's Trust for Endangered
569 Species, the Morris Animal Foundation (D12ZO-002). JS and MCF were supported by the
570 Leverhulme Trust (RPG-2014-273) and the Morris Animal Foundation (D16ZO-022). FB
571 was supported by the ERC (grant ERC 260801 – Big_Idea). DMA was funded by Wellcome
572 Trust Grant 099202. JV was supported by the Hungarian Scientific Research Fund (OTKA
573 K77841) and Bolyai János Research Scholarship, Hungarian Academy of Sciences
574 (BO/00579/14/8). DG was supported by the Conservation Leadership Programme (grant
575 0134010) with additional assistance from F. Gebresenbet, R. Kassahun and S.P. Loader. CS-
576 A was supported by Fondecyt N°11140902 and 1181758. TD-B was supported by the Royal
577 Geographical Society and the Royal Zoological Society of Scotland with assistance from
578 Mareike Hirschfeld and the Budongo Conservation Field Station. BW was supported by the
579 National Research Foundation of Korea (2015R1D1A1A01057282). LFT was supported by
580 FAPESP (#2016/25358-3) and CNPq (#300896/2016-6). LB (Berger), LFS and RJW were
581 supported by the Australian Research Council (FT100100375, DP120100811). AAC was
582 supported by a Royal Society Wolfson Research Merit award. JH, AL and SM were funded
583 by the Swedish Research Council Formas (grant no. 2013-1389-26445-20). CW was funded
584 by the National Research Foundation, South Africa. TYJ and TSJ acknowledge a National
585 Science Foundation Grant (DEB-1601259). WEH was funded by the NSERC Strategic and
586 Discovery grant programs.
587

588 **Author contributions:** All authors contributed ideas, data and editorial advice. S.J.O., A.R.,
589 R.C.F., K.A.M., B.B., and M.C.F. conducted analyses. G.M.R., T.W.J.G and L.B. conducted
590 disease experiments. S.J.O., F.B., T.W.J.G. and M.C.F. wrote the paper with input from all
591 authors.

592

593 **Competing interests:** KAM sits on an expert panel at the European Food Safety Authority
594 addressing the risks of importation and spread of the salamander chytrid *Batrachochytrium*
595 *salamandrivorans*, a species of fungus that is the closest known relative to the pathogen
596 addressed in this manuscript.

597

598 **Data availability:** Sequences have been deposited in the National Center for Biotechnology
599 Information (NCBI) Sequence Read Archive (SRA). All sequences are available from NCBI
600 BioProject accession PRJNA413876
601 (<https://www.ncbi.nlm.nih.gov/bioproject/PRJNA413876>). The supplementary materials
602 contain additional data. Phylogenetic trees are available from TreeBASE, project accession
603 url: <http://purl.org/phylo/treebase/phyloids/study/TB2:S22286>. A browsable version of the
604 phylogeny and metadata in Fig. 1B is accessible at: <https://microreact.org/project/GlobalBd>

605 **List of supplementary materials:**

606 Materials and Methods

607 Figs. S1 to S15

608 Tables S1 to S5

609 Data S1 to S3

610 References (45-92)

611 **Tables:**

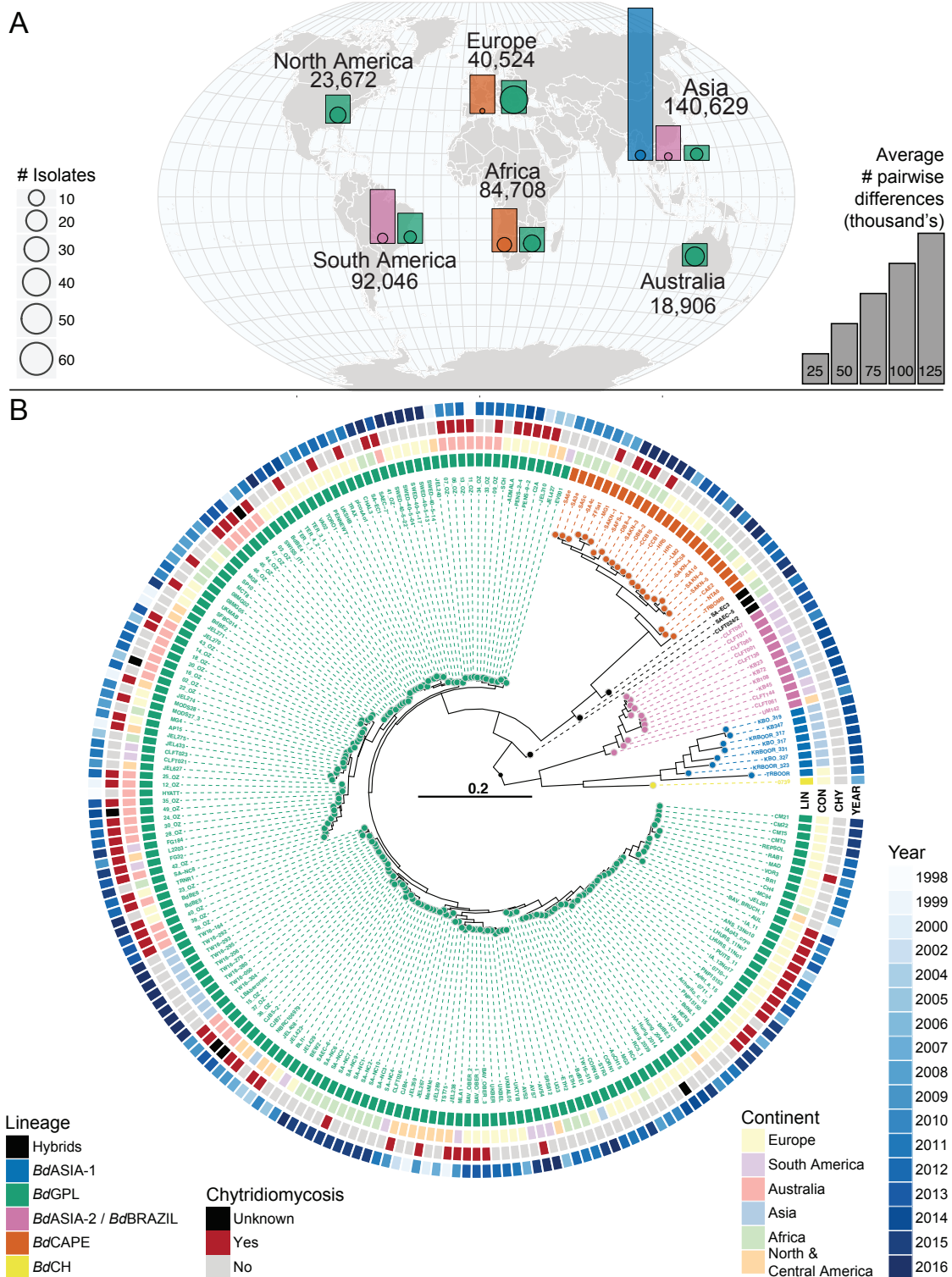
Lineage	Number of Isolates	Total segregating sites	Average pairwise-segregating sites	Total homozygous segregating sites	Average pairwise-homozygous segregating sites	π	Tajima's D
<i>Bd</i> ASIA-1	8	327,996	142,437	108,353	21,716	0.0044	0.2540
<i>Bd</i> ASIA-2 / <i>Bd</i> BRAZIL	12	148,021	51,069	48,722	6,216	0.0018	0.9825
<i>Bd</i> CAPE	24	146,466	38,881	53,884	4,977	0.0016	0.3143
<i>Bd</i> GPL	187	127,770	26,546	68,493	3,101	0.0009	0.9792

612

613 **Table 1.** Comparison of common genetic diversity measures among *Batrachochytrium*
614 *dendrobatidis* lineages. Total segregating sites for each lineage include all segregating sites
615 where genotype calls were made in at least half of the isolates. Average pairwise-segregating
616 sites is the average number of sites with different genotypes between all pairs of isolates
617 within a lineage. Total homozygous segregating sites includes all sites within a lineage where
618 there is at least one homozygous difference between isolates. Average pairwise homozygous
619 segregating sites is the average number of sites with different homozygous genotypes
620 between all pairs of isolates within a lineage. Nucleotide diversity (π) is the mean of the per-
621 site nucleotide diversity. Tajima's D is reported as the mean over 1 kbp bins.

622

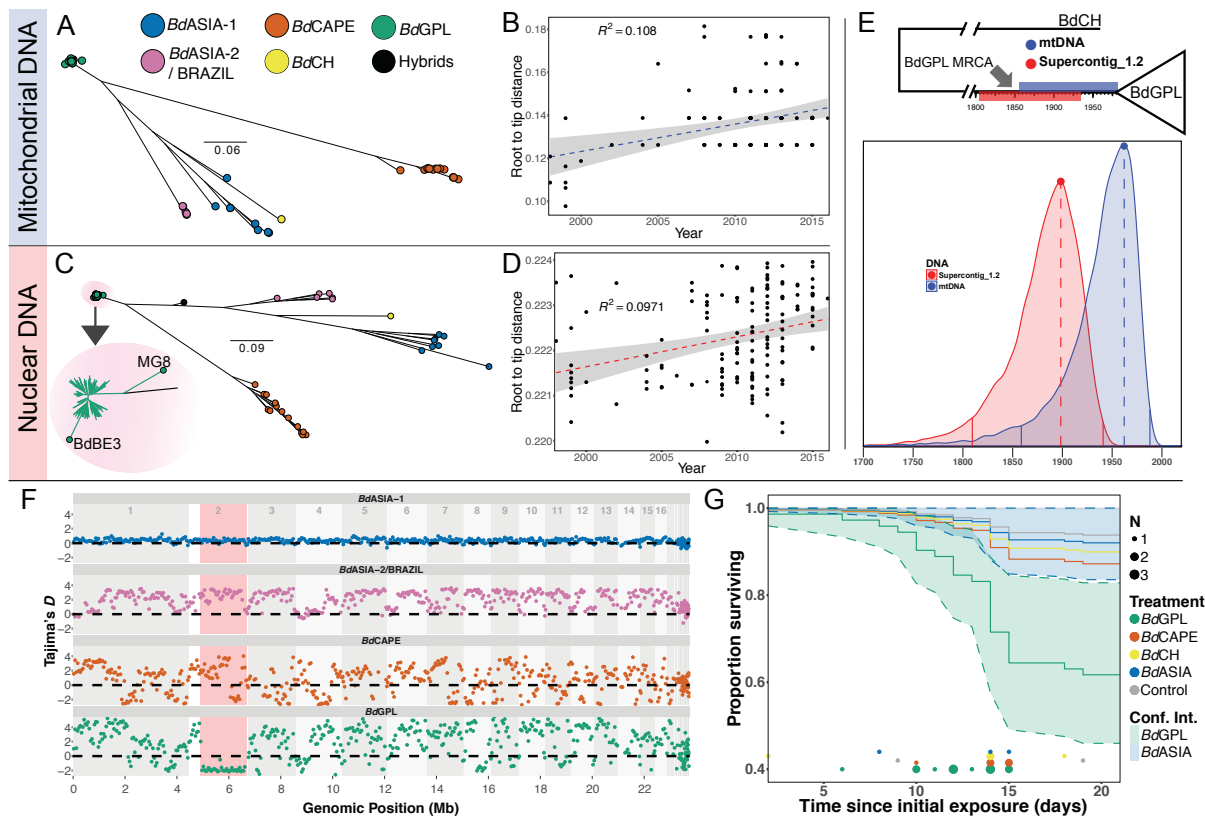
623 **Figures:**



624

625 **Fig. 1:** Genetic diversity and phylogenetic tree of a global panel of 234 *Batrachochytrium*
 626 *dendrobatidis* isolates. **A.** Map overlaid with bar charts showing the relative diversity of
 627 isolates found in each continent and by each major lineage (excluding isolates from traded
 628 animals). The bar heights are the average number of segregating sites between all pairwise

629 combinations of isolates of each lineage in each continent (therefore only lineages with two
630 or more isolates from a continent are shown). Outlined points at the base of each bar are
631 scaled by the number of isolates for each lineage in that continent. The numbers around the
632 outside of the globe are the average number of segregating sites between all pairwise
633 combinations of isolates grouped by continent. Colours denote lineage as given by the legend
634 in Fig 1B. **B.** Midpoint rooted radial phylogeny supports four deeply diverged lineages of *B.*
635 *dendrobatidis*: *BdASIA-1*; *BdASIA-2/BdBRAZIL*; *BdCAPE* and *BdGPL*. All major splits
636 within the phylogeny are supported by 100% of 500 bootstrap replicates. See Fig. S2 for tree
637 with full bootstrap support values on all internal branches.
638
639



640

641 **Fig. 2:** Dating the emergence of *BdGPL*. **A.** Maximum likelihood (ML) tree constructed from642 1,150 high quality SNPs found within the 178 kbp mitochondrial genome. **B.** Linear643 regression of root-to-tip distance against year of isolation for *BdGPL* isolates in

644 mitochondrial DNA phylogeny in panel A, showing significant temporal trend (F-statistic =

645 14.35, $p = 0.00024$). **C.** ML tree constructed from a 1.66 Mbp region of low recombination in646 Supercontig_1.2. Two *BdGPL* isolates, BdBE3 and MG8 fall on long branches away from647 the rest of the *BdGPL* isolates (see inset zoom), due to introgression from another lineage648 (*BdCAPE*; see Fig. 3B) and were excluded from the dating analysis. **D.** Linear regression of649 root-to-tip distance against year of isolation for *BdGPL* isolates from phylogeny in panel C,650 with significant temporal trend (F-statistic = 15.92, p -value = 0.0001). **E.** Top figure shows651 *BdGPL* and outgroup *BdCH*, with the 95% HPD estimates for MRCA for *BdGPL* from

652 mtDNA dating (blue) and nuclear DNA dating (red). Lower figure shows full posterior

653 distributions from tip dating models for mtDNA (blue) and partial nuclear DNA (red)

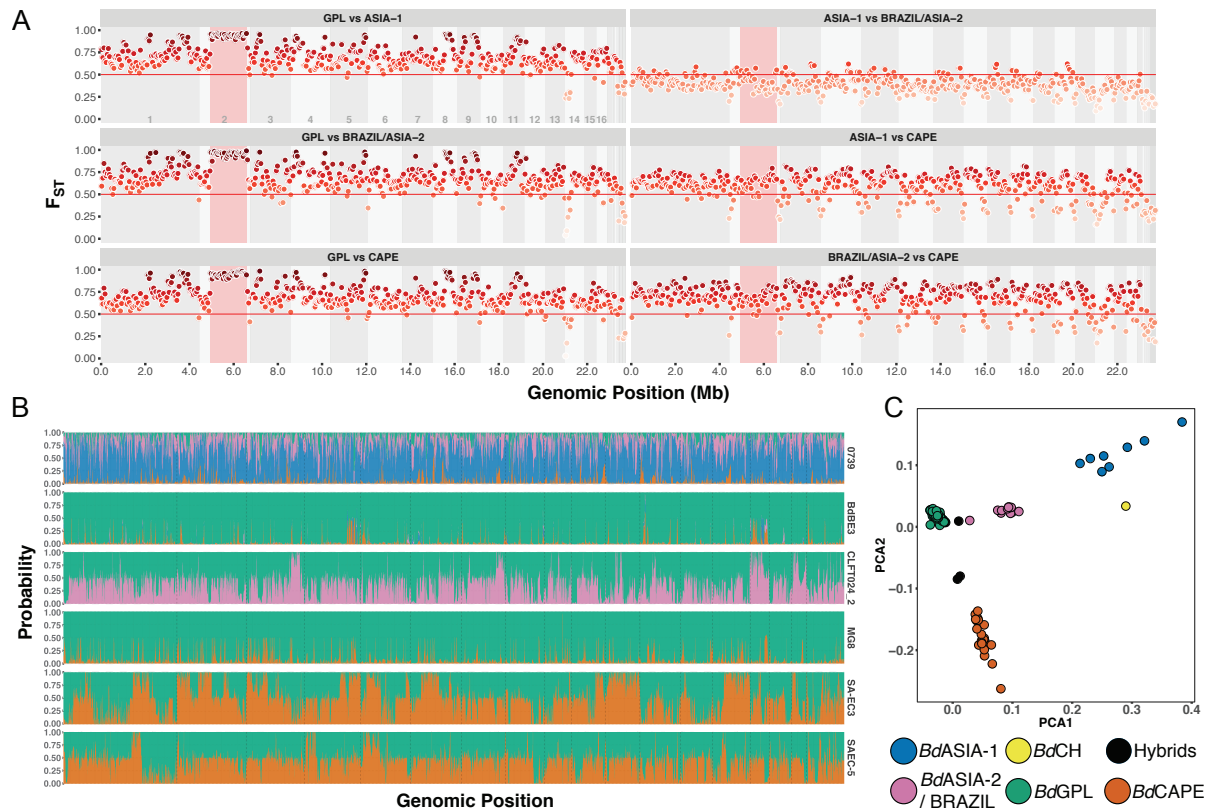
654 genomes. Solid vertical lines are limits of the 95% HPD. Dashed vertical lines denote the

655 maximal density of the posterior distributions. **F.** Sliding 10 kb, non-overlapping window656 estimates of Tajima's D for each of the main *B. dendrobatidis* lineages. The region657 highlighted in red is the low recombination segment of Supercontig_1.2. **G.** Survival curves658 for *Bufo bufo* metamorphs for different *B. dendrobatidis* treatment groups: *BdASIA-1* (blue);659 *BdCAPE* (orange); *BdCH* (yellow); *BdGPL* (green) and Control (grey). Confidence intervals

660 are shown for *Bd*GPL and *Bd*ASIA-1, showing no overlap by the end of the experiment.
661 Instances of mortalities in each treatment group are plotted along the x-axis, with points
662 scaled by number of mortalities at each interval (day).

663

664



665

666

667

668

669

670

671

672

673

674

675

676

677

678

Fig. 3: F_{ST} and site-by-site STRUCTURE analysis. **A.** Non-overlapping, 10 kb sliding window of F_{ST} between lineages. The region highlighted in red is Supercontig_1.2:500,000-2,160,000 low recombination region. **B.** Site-by-site analysis of population ancestry for a random selection of 9,905 SNPs. Results show those isolates found to be either hybrid (SA-EC3, SA-EC5 and CLFT024/2), or with significant introgression from non-parental lineages (isolates BdBE3 and MG8) or a chimera of un-sampled diversity, likely originating from East Asia (0739, the *BdCH* isolate). Each column represents a bi-allelic SNP position. The column is coloured according to the joint-probability of either allele copy arising from one of four distinct populations. Colours represent assumed parental lineages as given in Fig. 3C. **C.** Principle Components Analysis (PCA) of 3,900 SNPs in linkage equilibrium. Each point represents an isolate, coloured by phylogenetic lineage. The isolates separate into clearly defined clusters. The axes plot the first and second principle components.

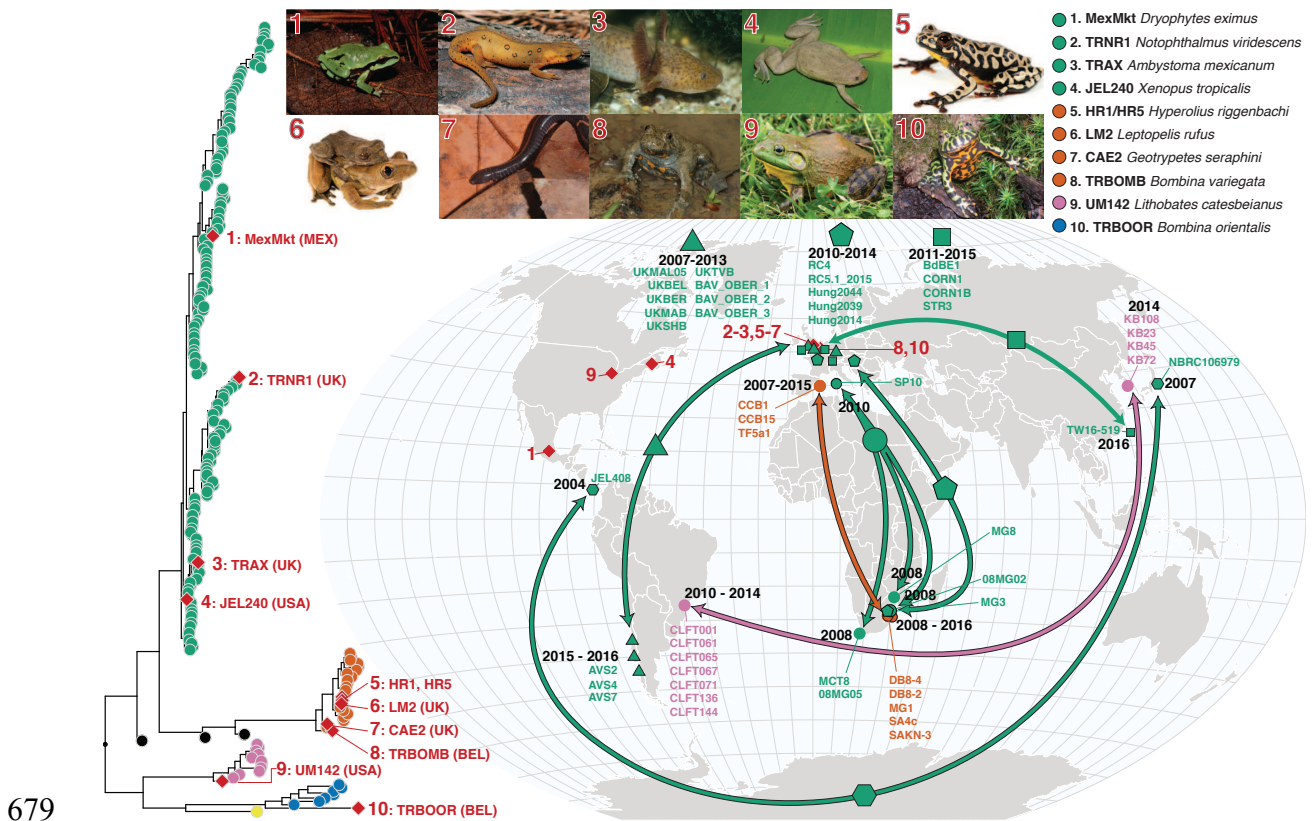


Fig. 4: Genotypes of *Bd* isolated from infected amphibians in the international trade and phylogenetically linked genotypes from segregated geographic localities. The red diamonds on the phylogeny indicate isolates recovered from traded animals. Their geographic location is displayed by the red diamonds on the map. The red numbers link each trade isolate to the relevant picture of the donor host species atop the figure panel and their placement in the phylogeny. The arrows on the map link geographically separated isolates which form closely related phylogenetic clades with high bootstrap support ($\geq 90\%$). Each clade is denoted by a different shape point on the map with the names of isolates within each clade displayed on the map. The dates displayed indicate the sampling time-frame for each clade. The phylogenetic position of each clade is displayed in Figs S10-14. The colours of points and arrows on the map indicate lineage according to the legend in Fig 1. A browsable version of this phylogeny can be accessed at <https://microreact.org/project/GlobalBd>. Photo credits: (1) *Hyla eximia* Ricardo Chaparro, (2) *Notophthalmus viridescens* Patrick Coin / CC-BY-SA 2.5, (3) *Ambystoma mexicanum* Henk Wallays, (4) *Xenopus tropicalis* Daniel Portik, (5) *Hyperolius riggenbachi* and (6) *Leptopelis rufus* Brian Freiermuth, (7) *Geotrypetes seraphini* Peter Janzen, (8) *Bombina variegata* and (9) *Rana catesbeiana* and (10) *Bombina orientalis* Frank Pasmans